AIAA JOURNAL
Vol. 40, No. 2, February 2002

Study of the Error and Efficiency of Numerical Schemes for Computational Aeroacoustics

James R. DeBonis*
NASA John H. Glenn Research Center at Lewis Field, Cleveland, Ohio 44135
and
James N. Scott†
The Ohio State University, Columbus, Ohio 43210

Two types of high-order numerical schemes suitable for computational aeroacoustics are examined. Truncation error, efficiency, and the consequence of disparate temporal and spatial accuracy are discussed. The Gottlieb–Turkel 2-4 predictor-corrector scheme and two Runge–Kutta schemes (4-4 and 4-6) are used to solve the one-dimensional inviscid convection of a Gaussian pulse. For schemes with lower-order time stepping, the truncation error caused by the time stepping dominates the solution for optimum time steps. Reducing the time step can effectively increase the order of accuracy to that of the spatial discretization. However, this increased accuracy is balanced by an increase in the computational cost. The uniformly fourth-order-accurate Runge–Kutta scheme proves to be superior to the second-order temporal and fourth-order spatial accurate Gottlieb–Turkel scheme in terms of truncation error and computational efficiency. Increasing the spatial accuracy of the Runge–Kutta scheme to sixth order does not improve the efficiency of the scheme. To illustrate the relevance to a representative multi-dimensional problem, the Gottlieb–Turkel 2-4 and Runge–Kutta 4-4 schemes are then used to solve the unsteady axisymmetric Navier–Stokes equations for a supersonic jet. For this case the Runge–Kutta scheme provides better resolution of large-scale structures and requires less computational time.

Nomenclature

A	=	linearizing coefficient
$\boldsymbol{D}$	=	spatial operator
D_j	=	jet diameter
E	=	flux vector in axial direction
e_t	=	total energy per unit mass
F	=	flux vector in radial direction
f	=	one-dimensional flux
H	=	axisymmetric source term vector
l_2	=	residual error
p	=	pressure
$\boldsymbol{p}$	=	order of accuracy
Q	=	conservation variable vector
q	=	heat flux
Re_j	=	Reynolds number based on jet diameter
r	=	radial coordinate
T	=	temperature
t	=	time
u	=	axial velocity
v	=	radial velocity
x	=	axial coordinate
γ	=	ratio of specific heats
Δt	=	time step
Δx	=	spatial step
μ	=	dynamic viscosity
ρ	=	density
σ	=	stress tensor

Subscripts

ex	=	exact
j	=	jet
v	=	viscous
0	=	stagnation/total condition
∞	=	freestream

Superscript

$*$	=	intermediate time

Introduction

COMPUTATIONAL methods are being increasingly used to solve aeroacoustic problems. Many computational aeroacoustics (CAA) analyses employ large-eddy simulations (LES) and direct numerical simulations (DNS). These types of analyses impose strict requirements on the numerical scheme. Both types of simulations are inherently unsteady, requiring a time accurate/unsteady analysis. In addition, to capture the turbulent scales and acoustic waves high spatial accuracy is desired.

To obtain this accuracy, meshes on the order of millions of grid points are required. As a result, accuracy comes at a very large cost in terms of computational time; run times of several months are common for realistic problems. Morris et al.[1] performed an LES analysis of a Mach 2.1 jet that used over 2 million grid points and 1000 CPU hours. A LES analysis of a low-speed jet, Mach 0.4, by Zhao et al.[2] used 3.6 million grid points and 4000 CPU hours. A hybrid Reynolds averaged Navier–Stokes (RANS)/LES analysis of a compressible mixing layer by Georgiadis et al.[3] used 1.9 million grid points and 2000 CPU hours. Freund's benchmark DNS data on low-Reynolds-number jets[4,5] were obtained on grids of over 20 million points (run times were not reported).

Numerous numerical schemes have been developed for and applied to CAA problems. Recent work has focused on compact and dispersion relation preserving schemes.[6–9] A great deal of effort has focused on increasing the spatial accuracy of the numerical scheme in order to reduce the grid requirements and hence lower the computational cost. Because CAA involves the computing the propagation of sound waves, a popular method for assessing the accuracy of these schemes is the Fourier analysis of the spatial discretization.[10] The accuracy of these schemes is commonly expressed in terms

Received 12 February 2001; revision received 27 August 2001; accepted for publication 31 August 2001.

*Aerospace Engineer, Nozzle Branch. Senior Member AIAA.
†Associate Professor, Department of Aerospace Engineering and Aviation. Associate Fellow AIAA.

of the number of mesh points per wavelength required to resolve a wave. The more traditional classification of numerical schemes is done by order of accuracy, with the spatial discretization considered separately from the temporal discretization. For example, a 2-4 scheme is second-order accurate in time and fourth-order accurate in space. However, judging a numerical scheme based solely on its spatial error, via a points per wavelength requirement or order of accuracy, disregards two important factors: the effect of the temporal discretization on the error and the efficiency or computational cost of the scheme. These factors become critical when the schemes are applied to large-scale computations such as those just cited.

An examination of numerous numerical schemes was presented in the proceedings of the first NASA-sponsored CAA workshop.[11] This workshop examined the schemes on several benchmark problems relevant to CAA. However, the schemes were examined only qualitatively in terms of numerical error. Typically only one spatial discretization (a single grid) was used, and no attempt at quantifying computational efficiency was made. For large-scale LES and DNS the efficiency is an important consideration when choosing or developing a numerical scheme. This paper examines the behavior of two types of commonly used schemes in terms of numerical error and computational cost on a one-dimensional model equation. To examine the relevance of the one-dimensional results on a multidimensional problem, the schemes are applied to an unsteady Navier–Stokes computation of a supersonic axisymmetric jet. Particular attention is paid to how the spatial and temporal errors affect the overall order of accuracy and efficiency of the scheme.

Numerical Methods

The numerical schemes will be presented in terms of the inviscid one-dimensional convection equation given by

$$\frac{\partial u}{\partial t} + \frac{\partial f}{\partial x} = 0 \tag{1}$$

where $f = f(u)$.

Gottlieb–Turkel Scheme

The first scheme examined is the Gottlieb–Turkel 2-4 scheme.[12] It is a variant of MacCormack's predictor-corrector method.[13] MacCormack's method was second-order accurate in both time and space. Gottlieb and Turkel extended the spatial accuracy to fourth-order while maintaining second-order temporal accuracy. The scheme was developed 25 years ago, but is still widely used for CAA applications. This method is robust, easy to implement, and requires only two storage locations for each dependent variable (2-N storage):

$$u_i^* = u_i^n - \frac{1}{6}\frac{\Delta t}{\Delta x}\left(-f_{i+2}^n + 8f_{i+1}^n - 7f_i^n\right) \tag{2a}$$

$$u_i^{n+1} = \frac{1}{2}\left[u_i^n + u_i^* - \frac{1}{6}\frac{\Delta t}{\Delta x}\left(7f_i^* - 8f_{i-1}^* + f_{i-2}^*\right)\right] \tag{2b}$$

The leading terms in the truncation error for the Gottlieb–Turkel scheme are

$$-\frac{(\Delta t)^2}{6}\frac{\partial^3 u}{\partial t^3} + \frac{(\Delta x)^4}{30}\frac{\partial^5 f}{\partial x^5} - \frac{\Delta t(\Delta x)^2}{18}A\frac{\partial^4 f}{\partial x^4} \tag{3}$$

where f is linearized as $f = Au$. In addition to retaining the second-order time accuracy, it is important to note that the cross term is dissipative and is scaled by $\Delta t(\Delta x)^2$.

Runge–Kutta Schemes

As seen with the Gottlieb–Turkel scheme, all higher-order variants of MacCormack's method maintain second-order time accuracy. To quantify the detrimental effect of the disparity in temporal and spatial accuracy, a uniformly fourth-order scheme was desired. To increase the order of time accuracy, an alternative method for time advancement, the Runge–Kutta scheme, was necessary.

Runge–Kutta schemes are a popular family of numerical schemes with higher-order temporal accuracy. These multistage schemes can be formulated for any order of accuracy. The number of stages in the scheme is equal to or greater than the desired order of accuracy. The standard fourth-order Runge–Kutta scheme used by Jameson[14] is a four-stage algorithm and requires storage locations for each variable (2-N storage). Several researchers[15–18] have developed alternative Runge–Kutta schemes that have a lower dispersion error than the standard scheme, leading to greater stability and accuracy. To accomplish this, additional stages are required. The additional stages provide a means to impose the additional constraints necessary to minimize the error. All of the alternative schemes are based on a general M-stage 2-N storage formulation given by

$$\mathrm{d}u_m = \alpha_m\,\mathrm{d}u_{m-1} + \Delta t\boldsymbol{D}(u_{m-1}) \tag{4a}$$

$$u_m = u_{m-1} + \beta_m\,\mathrm{d}u_m \tag{4b}$$

for $m = 1, \ldots M$, and where $u_0 = u^n$ and $u_M = u^{n+1}$. The coefficient α_1 is typically set to zero for the algorithm to be self-starting. The operator $\boldsymbol{D}$ is the spatial finite difference operator.

Carpenter and Kennedy's five-stage fourth-order scheme[15] was chosen for its fourth-order accuracy, low number of stages, and ease of programming. The coefficients for the scheme are given in Table 1.

Table 1 Coefficients for fourth-order low-dispersion Runge–Kutta scheme

Stage, m	α_m	β_m
1	0.00000000000	0.1496590219993
2	−0.41789047450	0.3792103129999
3	−1.192151694643	0.8229550293869
4	−1.697784692471	0.6994504559488
5	−1.514183444257	0.1530572479681

Runge–Kutta 4-4 Scheme

For a uniformly fourth-order scheme, $\boldsymbol{D}(u)$ would be a fourth-order finite difference stencil for $-\partial f/\partial x$. A central difference stencil for $\partial f/\partial x$ is used here:

$$\frac{\partial f}{\partial x} = \frac{-f_{i+2} + 8f_{i+1} - 8f_{i-1} + f_{i-2}}{12(\Delta x)} \tag{5}$$

The leading terms in the truncation error are

$$-\frac{(\Delta t)^4}{300}\frac{\partial^5 u}{\partial t^5} + \frac{(\Delta x)^4}{30}\frac{\partial^5 f}{\partial x^5} - \frac{\Delta t(\Delta x)^4}{30}A\frac{\partial^6 f}{\partial x^6} \tag{6}$$

The error caused by the spatial discretization is identical to that of the Gottlieb–Turkel scheme, but the temporal error and the cross term have been altered.

Runge–Kutta 4-6 Scheme

Many schemes currently in use combine fourth-order Runge–Kutta time stepping with higher-order spatial operators. To mimic these schemes a 4-6 scheme was created using a sixth-order central difference:

$$\frac{\partial f}{\partial x} = \frac{f_{i+3} - 9f_{i+2} + 45f_{i+1} - 45f_{i-1} + 9f_{i-2} - f_{i-3}}{60(\Delta x)} \tag{7}$$

The leading terms in the truncation error for this scheme are

$$-\frac{(\Delta t)^4}{300}\frac{\partial^5 u}{\partial t^5} - \frac{(\Delta x)^6}{140}\frac{\partial^7 f}{\partial x^7} + \frac{\Delta t(\Delta x)^6}{140}A\frac{\partial^8 f}{\partial x^8} \tag{8}$$

One-Dimensional Model Problems

Two one-dimensional problems were used to test the accuracy and efficiency of the schemes. Both are based on the model equation just given [Eq. (1)].

Problem Descriptions

Problem 1

The first problem, from the first NASA CAA workshop[11] is the linear convection of a Gaussian pulse, where $f = u$. The initial condition is given by

$$u(x, 0) = u_0(x) = \tfrac{1}{2}\exp[-\ln(2)(x/3)^2] \tag{9}$$

The domain is $-20 \le x \le 450$, and the solution is run for $0 \le t \le 400$. An exact solution to this problem exists and is given by

$$u_{\mathrm{ex}}(x, t) = u_0(x - t) \tag{10}$$

Problem 2

The second problem is nonlinear, where $f = \frac{1}{2}u^2$. The initial conditions and simulation time are set so that a smooth final solution is obtained. The initial condition is

$$u(x, 0) = u_0(x) = \tfrac{1}{8}\exp[-\ell n(2)(x/10)^2] \tag{11}$$

The domain is $-50 \le x \le 50$, and the solution is run for $0 \le t \le 100$. A numerical approximation to the exact solution is obtained using the method of characteristics.

Results

All of the one-dimensional computations were run using 64-bit precision on an Apple Macintosh Powerbook G3 computer with a 266-MHz PowerPC G3 processor.

The error of the numerical scheme was measured by the l_2 norm, which is computed as follows:

$$l_2 = \left[\frac{x_{\max} - x_{\min}}{n-1}\sum_{i=1}^{n}\left(u_i - u_{\mathrm{ex}_i}\right)^2\right]^{\frac{1}{2}} \tag{12}$$

For each problem the numerical schemes were run to determine the maximum stable time step. Then, each scheme was run at a number of different values of $\Delta t/\Delta x$ as the spatial step was halved.

Problem 1

The exact solution to the linear problem is presented in Fig. 1. All of the schemes approach the exact solution as Δt and Δx approach zero. Error from the Gottlieb–Turkel scheme is plotted vs time step and spatial step (Fig. 2). The terminal slope of the line $\boldsymbol{p}$ indicates the order of accuracy of the scheme and is listed in the plot legend. The error is plotted vs the time step in Fig. 2a. As expected from the truncation error analysis, the scheme is second order. When the error is plotted vs the spatial step (Fig. 2b), the scheme retains its second-order accuracy. The error caused by the time discretization dominates the problem. This can be seen by the collapsing of the data when plotted vs the time step and not the spatial step size. Only where the time step is much smaller than the spatial step does the scheme behave as a fourth-order scheme. To obtain fourth-order behavior from the Gottlieb–Turkel scheme, the error term from the time step must be reduced at the same rate as the error term from the spatial step. To accomplish this, the time step must be reduced by a factor of $\frac{1}{4}$ as the spatial step is reduced by $\frac{1}{2}$. In other words, $\Delta t/(\Delta x)^2$ is held constant. Figure 3 verifies that when adjusting the time step in this manner fourth-order accuracy is obtained.

The error for Runge–Kutta 4-4 scheme is plotted in Fig. 4. These data indicate that the scheme is truly a fourth-order-accurate scheme. In addition, except for the highest value of $\Delta t/\Delta x$ where the time error term dominates, the error is dominated by the spatial discretization.

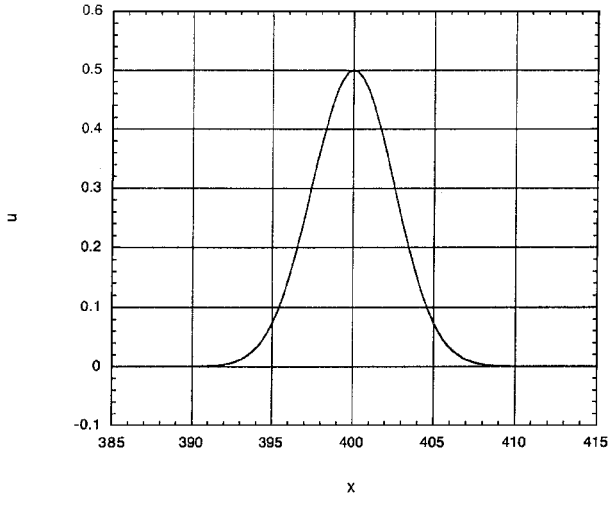

Fig. 1 Solution to inviscid linear convection problem at $t = 400$.

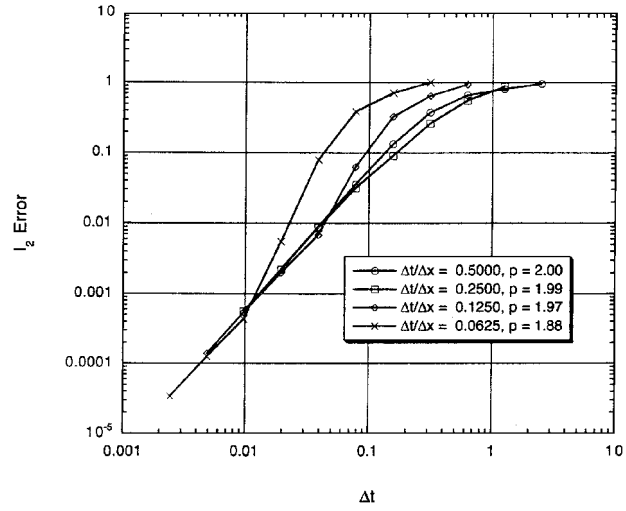

a) Temporal error

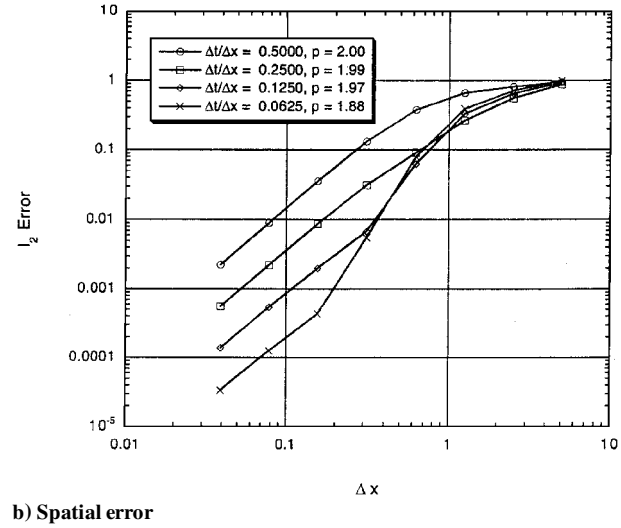

b) Spatial error

Fig. 2 Error of Gottlieb–Turkel 2-4 scheme for the linear problem.

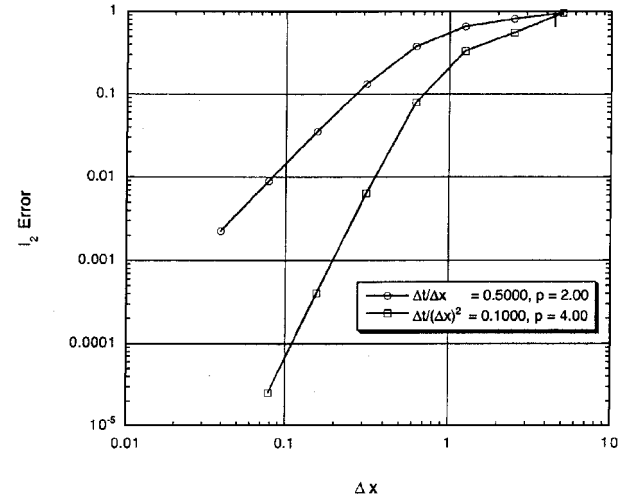

Fig. 3 Improved spatial error of Gottlieb–Turkel 2-4 scheme for the linear problem.

Results for the Runge–Kutta 4-6 scheme (Fig. 5) are similar to those for the Gottlieb–Turkel 2-4 scheme. For the larger time steps the error caused by the lower-order time discretization dominates the problem, making the scheme fourth-order accurate. By reducing the error from the time step at the same rate as the error from the spatial step, sixth-order accuracy can be obtained (Fig. 6). For this scheme this is done by reducing the time step by a factor of $\sqrt{2}/4$ as the spatial step is reduced by $\frac{1}{2}$. Here $(\Delta t)^2/(\Delta x)^3$ is held constant.

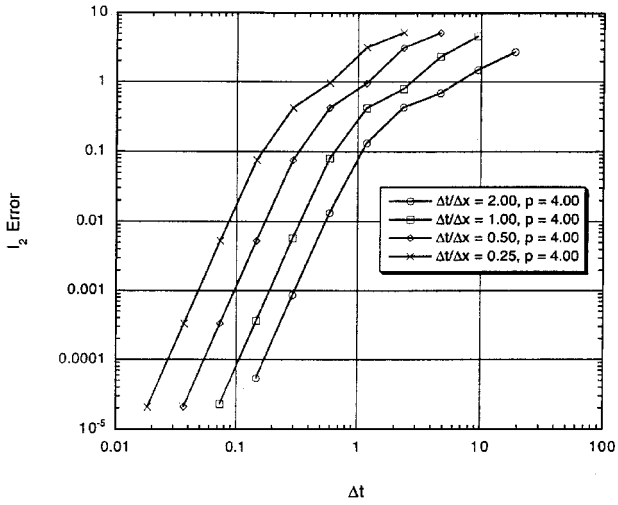

a) Temporal error

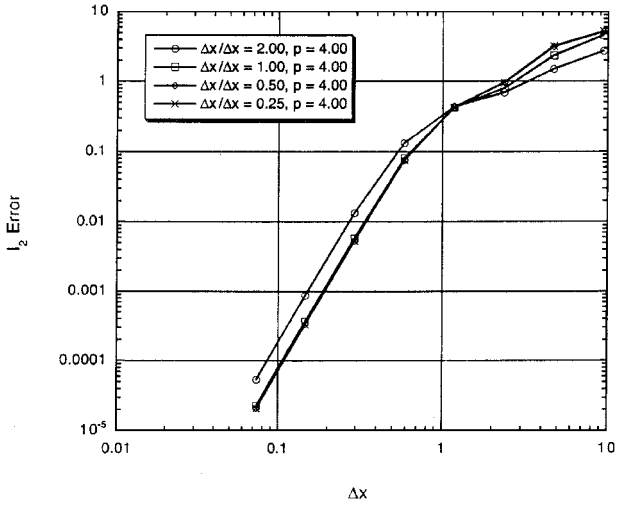

b) Spatial error

Fig. 4 Error of low-dispersion Runge–Kutta 4-4 scheme for the linear problem.

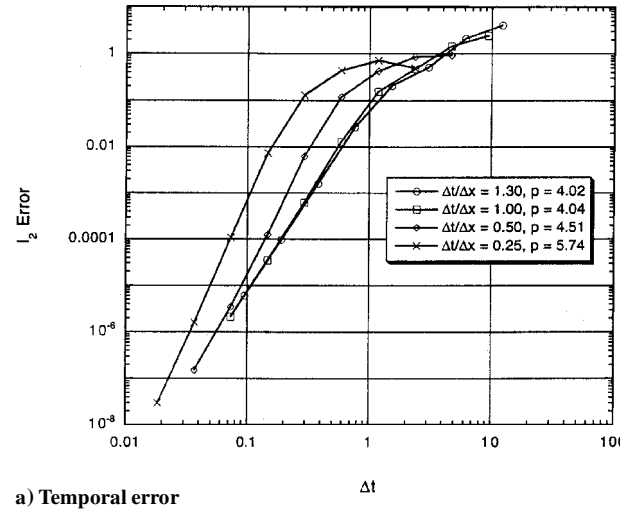

a) Temporal error

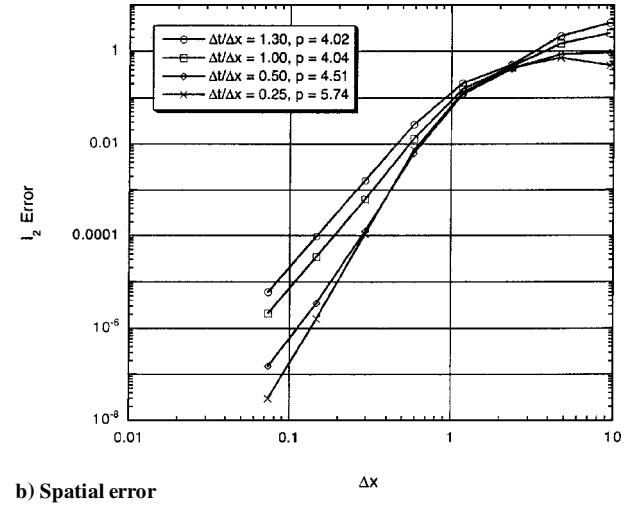

b) Spatial error

Fig. 5 Error of low-dispersion Runge–Kutta 4-6 scheme for the linear problem.

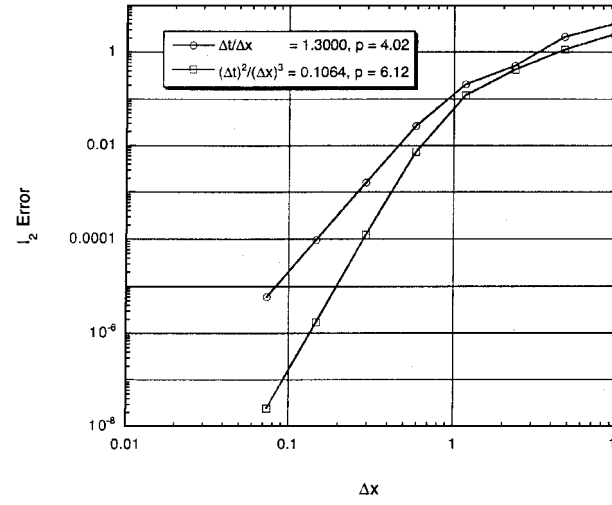

Fig. 6 Improved spatial error of low-dispersion Runge–Kutta 4-6 scheme for the linear problem.

The efficiency of a numerical scheme can be seen by comparing the l_2 error against the time required to obtain that error level. The schemes are compared at their maximum stable time step, to provide maximum efficiency. Figure 7 shows that the Runge–Kutta schemes are clearly more efficient than the Gottlieb–Turkel scheme. Runge–Kutta achieves error levels below 10^{-2} in at least an order of magnitude less time than the Gottlieb–Turkel scheme. This result is caused by the lower truncation error and larger allowable time step of the Runge–Kutta scheme. The Runge–Kutta 4-6 scheme has no advantage over the Runge–Kutta 4-4 scheme caused by the dominance of the time discretization error. Results for Gottlieb–Turkel 2-4 and Runge–Kutta 4-6 schemes are also shown when they were run to achieve fourth- and sixth-order accuracy, respectively. The data indicate that there is little or no benefit of reducing the time step to achieve the higher-order accuracy of the spatial discretization. The benefit of the higher-order accuracy is balanced by the increased computational cost.

Problem 2

The exact solution to the smooth nonlinear problem is presented in Fig. 8. Error data for this problem are shown in Figs. 9–14. The results from the nonlinear analysis are very similar to the linear case. Specifically, the lower-order temporal error of the Gottlieb–Turkel 2-4 and Runge–Kutta 4-6 schemes dominate the results at the larger time steps and render the schemes second- and fourth-order, respectively. Reducing the time step of these schemes can increase the order of accuracy to that of the spatial discretization (Figs. 10 and 13) with a corresponding increase in computational cost (Fig. 14). The higher-order Runge–Kutta schemes are more efficient than the Gottlieb–Turkel scheme. Because of the increased cost and fourth-order temporal accuracy, the 4-6 is not more efficient than the 4-4 scheme.

Axisymmetric Jet Analysis

The results of the preceding analysis indicate that a proper balance of the truncation error caused by the temporal and spatial discretizations is a key component to the accuracy and efficiency of a numerical scheme and could be important for CAA analyses,

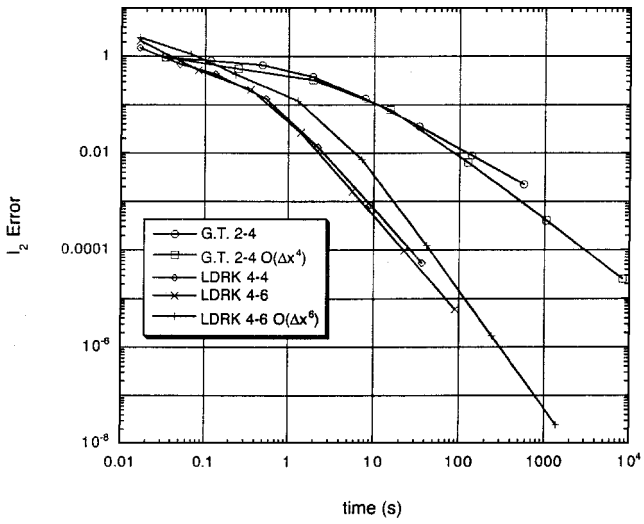

Fig. 7 Efficiency of the numerical schemes for the linear problem.

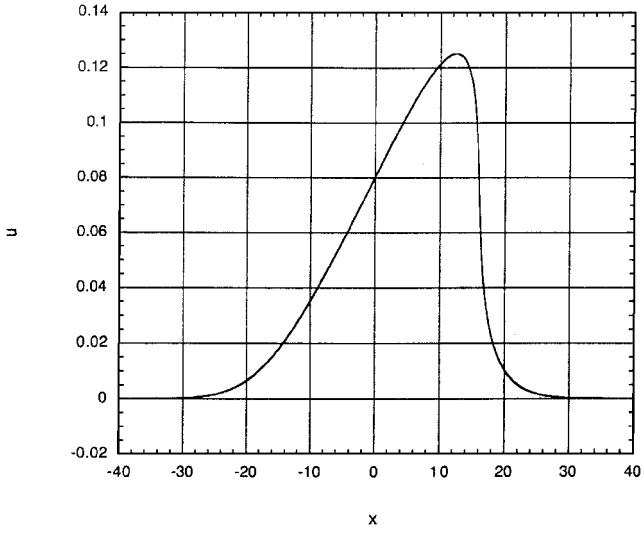

Fig. 8 Solution to inviscid nonlinear convection problem at $t = 100$.

where accurate resolution and computational cost are critical. To determine whether the one-dimensional results are relevant to multidimensional problems of in interest in CAA, the Gottlieb–Turkel 2-4 and Runge–Kutta 4-4 schemes were implemented in a Navier–Stokes solver for analysis of compressible nozzle flows. A solution filtering technique[19] was added to enhance stability. Both schemes were used in an axisymmetric analysis of a Mach 1.4 round jet to determine the effect of the numerical scheme on the resulting flowfield. The axisymmetric assumption ignores key physical processes present in the jet such as vortex stretching and flapping of the jet. In addition no subgrid scale modeling or turbulence modeling of any kind was used. These two simplifications prevent a realistic flow solution. But because the goal is to compare the effects of the numerical scheme on a computation that is representative of a DNS or LES analysis for a CAA application, they are reasonable and allow solutions to be obtained at a reduced computational cost.

The jet, which was examined experimentally by Panda and Seasholtz,[20] has a Reynolds number of 1.2×10^6 and an exit Mach number 1.4. The nozzle exhausted into quiescent air. Table 2 summarizes the nozzle and ambient conditions.

Problem Description

The axisymmetric Navier–Stokes equations that govern the flowfield of the jet are

Table 2 Nozzle and ambient conditions

Quantity	Symbol	Value
Ratio of specific heats	γ	1.4
Nozzle plenum pressure	p_{0_j}	312.41 kPa
Nozzle plenum temperature	T_{0_j}	300.0 K
Nozzle exit Mach number	M_j	1.395
Nozzle exit diameter	D_j	0.0254 m
Jet velocity	U_j	411.0 m/s
Ambient pressure	p_∞	98.863 kPa
Ambient temperature	T_∞	297.0 K
Reynolds number	Re_j	1.2×10^6

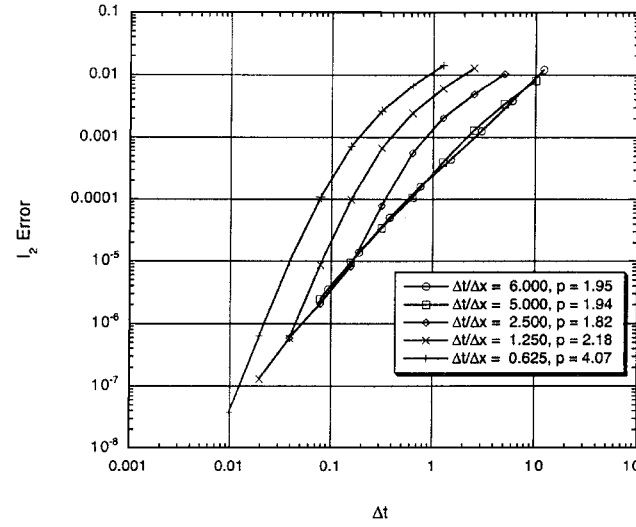

a) Temporal error

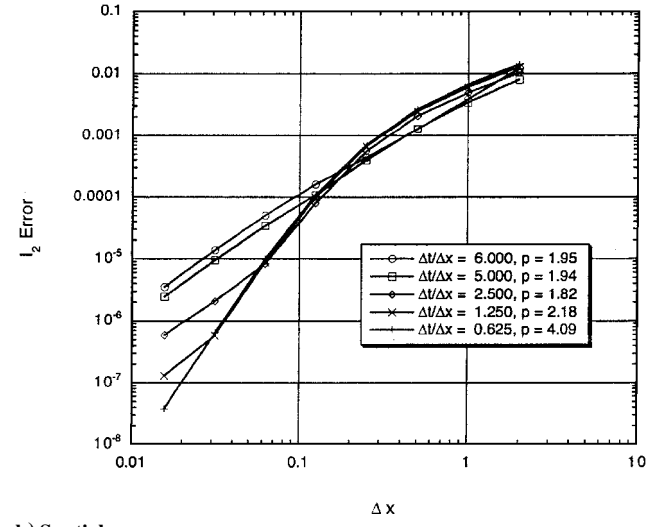

b) Spatial error

Fig. 9 Error of Gottlieb–Turkel 2-4 scheme for the nonlinear problem.

$$\frac{\partial Q}{\partial t} + \frac{\partial E}{\partial x} + \frac{\partial F}{\partial r} + H = \frac{\partial E_v}{\partial x} + \frac{\partial F_v}{\partial r} + H_v \qquad (13)$$

where

$$Q = \begin{bmatrix} \rho \\ \rho u \\ \rho v \\ \rho e_t \end{bmatrix}, \qquad H = \frac{1}{r}\begin{bmatrix} \rho v \\ \rho u v \\ \rho v^2 \\ (\rho e_t + p)v \end{bmatrix}$$

$$E = \begin{bmatrix} \rho u \\ \rho u^2 + p \\ \rho u v \\ (\rho e_t + p)u \end{bmatrix}, \qquad E_v = \begin{bmatrix} 0 \\ \sigma_{xx} \\ \sigma_{xr} \\ u\sigma_{xx} + v\sigma_{xr} - q_x \end{bmatrix}$$

Table 3 Axisymmetric scheme study data

Scheme	CFL	$(\Delta t U_j)/D_j$	Time	$\hat{u}_{\max}$	$\hat{v}_{\max}$	$k/\left(\frac{1}{2}U_j^2\right)$
Gottlieb–Turkel 2-4	0.6	3.9644×10^{-4}	1.00000	0.26033	0.18561	0.080193
Runge–Kutta 4-4	1.2	7.9288×10^{-4}	0.83523	0.26266	0.20305	0.096392

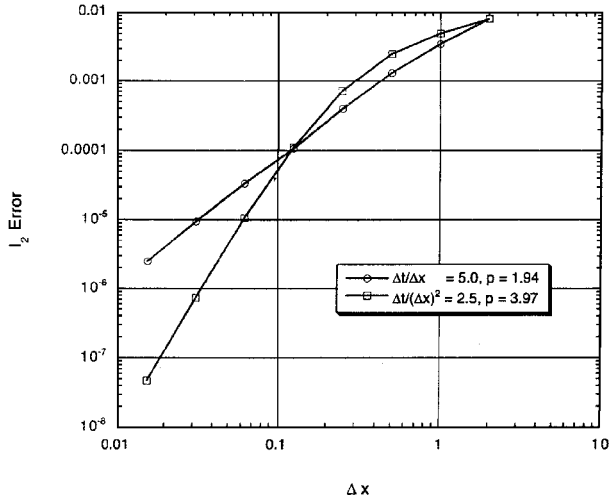

Fig. 10 Improved spatial error of Gottlieb–Turkel 2-4 scheme for the nonlinear problem.

$$F = \begin{bmatrix} \rho v \\ \rho v u \\ \rho v^2 + p \\ (\rho e_t + p)v \end{bmatrix}, \qquad F_v = \begin{bmatrix} 0 \\ \sigma_{rx} \\ \sigma_{rr} \\ u\sigma_{rx} + v\sigma_{rr} - q_r \end{bmatrix}$$

$$H_v = \begin{bmatrix} 0 \\ \sigma_{xr} - \frac{2}{3} r \frac{\partial}{\partial x}\left(\mu \frac{v}{r}\right) \\ \sigma_{rr} - \sigma_{\theta\theta} - \frac{2}{3}\mu\frac{v}{r} - \frac{2}{3} r \frac{\partial}{\partial r}\left(\mu \frac{v}{r}\right) \\ u\sigma_{xr} + v\sigma_{rr} - q_r - \frac{2}{3}\mu\frac{v^2}{r} - r\frac{\partial}{\partial r}\left(\frac{2}{3}\mu\frac{v^2}{r}\right) - r\frac{\partial}{\partial x}\left(\frac{2}{3}\mu\frac{uv}{r}\right) \end{bmatrix}$$

Solutions were obtained on a grid with 301 points in the axial direction and 129 points in the radial direction (Fig. 15). The domain extends 20 jet diameters downstream of the nozzle exit and 10 jet diameters above the centerline. The grid models both the external jet flowfield and the nozzle geometry, including the nozzle lip, in order to include the radial variation in the velocity profile caused by internal nozzle expansion, effects of under- or overexpansion of the nozzle flow and the effect of the nozzle lip geometry on the stability and growth of the mixing layer. The grid is clustered radially toward the mixing layer of the jet and axially toward the nozzle lip using hyperbolic tangent stretching. The minimum grid spacing occurs on the nozzle lip, which is defined using 29 points, and the cell aspect ratio is one.

Boundary conditions based on the local one-dimensional propagation of flow properties were used at the inflow and outflow. While the jet exited into quiescent air in the experiment, a Mach 0.05 freestream was used in the calculation to maintain well-posed boundary conditions. Total pressure and temperature were specified in the nozzle plenum. The use of an exit zone to damp reflected waves from the outflow boundary was explored in a previous study[21] and found not to be necessary for this case. Instead the static pressure was specified on the outer portion of the boundary, and the conditions were extrapolated near the jet centerline to allow for variation in the static pressure. Flow tangency was imposed on the jet axis, and the no-slip condition was imposed on solid surfaces.

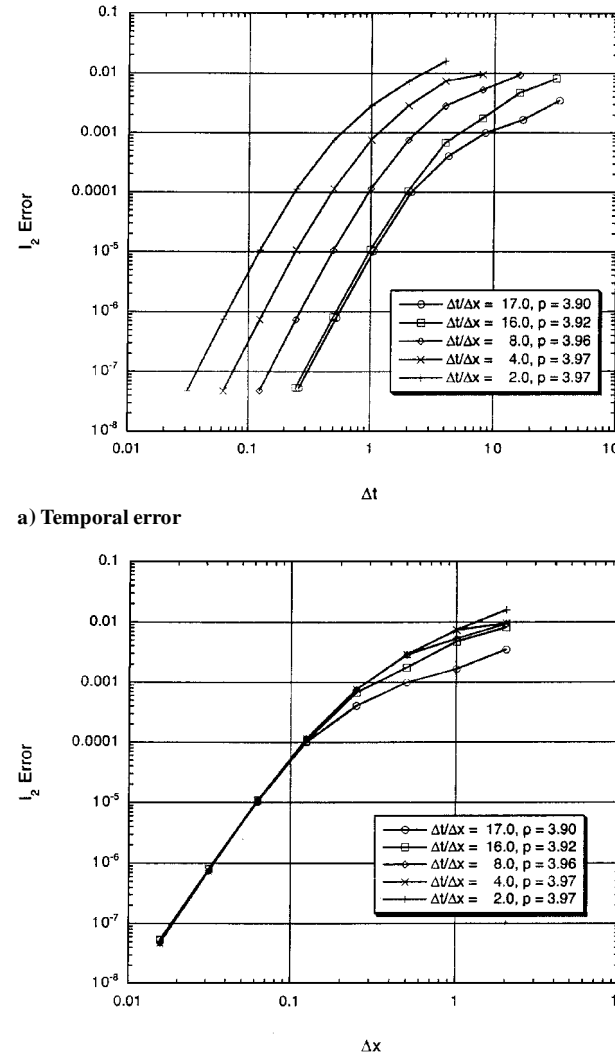

a) Temporal error

b) Spatial error

Fig. 11 Error of low-dispersion Runge–Kutta 4-4 scheme for the nonlinear problem.

Results

The solutions were run for two characteristic times (the time for an acoustic wave to pass through the solution domain) to establish proper initial conditions for obtaining turbulent statistics. The solutions were then run for an additional two characteristic times, and the flowfield was averaged. Both schemes were run using their maximum stable time step. The maximum stable time step is computed at every point in the flowfield using the inviscid Courant–Friedrichs–Lewy (CFL) condition.[22] The smallest of these stable time steps is then selected to advance the solution globally. The CFL numbers and corresponding time steps are listed in Table 3. Figure 16 shows the instantaneous entropy contours for the two schemes at the final time. The two flowfields are similar, but the Runge–Kutta scheme exhibits better resolution of the vortical structures. In addition, the initial vortex roll up of the shear layer occurs earlier using the Runge–Kutta 4-4 scheme, $x/D_j = 0.91$, compared to the Gottlieb–Turkel scheme, $x/D_j = 1.38$. Table 3 quantifies the results in terms of turbulent intensities $\hat{u}$ and $\hat{v}$ and turbulent kinetic energy $k/(\frac{1}{2}U_j^2)$. The Runge–Kutta scheme predicts higher maximum turbulent intensities and kinetic energy than the Gottlieb–Turkel

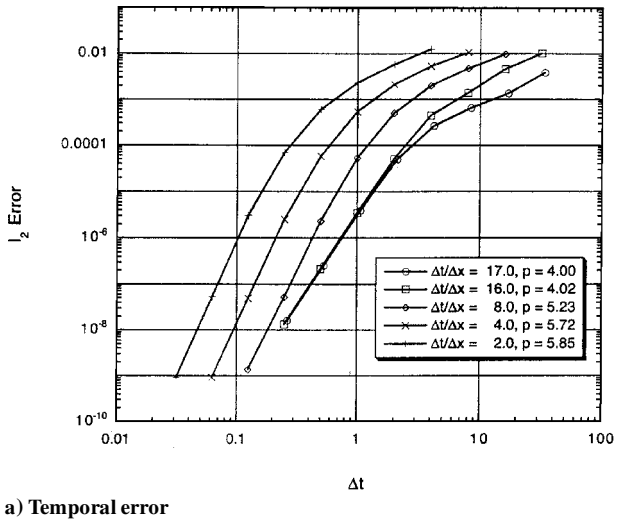

a) Temporal error

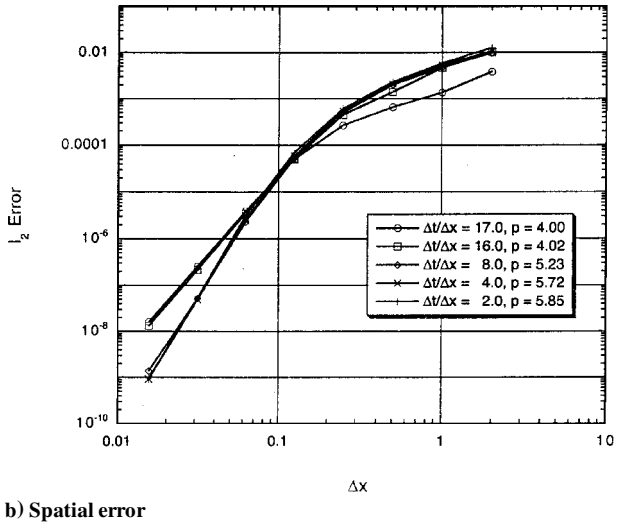

b) Spatial error

Fig. 12 Error of low-dispersion Runge–Kutta 4-6 scheme for the nonlinear problem.

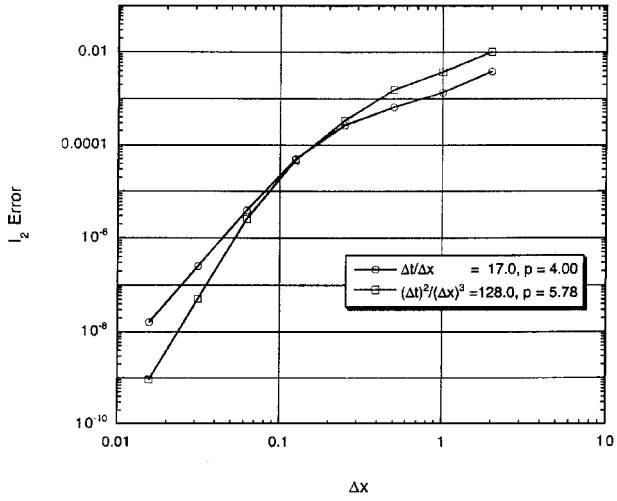

Fig. 13 Improved spatial error of low-dispersion Runge–Kutta 4-6 scheme for the nonlinear problem.

scheme, indicating better resolution of the flowfield. Because the error term caused by the spatial discretization is identical for both schemes, one must conclude that the differences between the solutions occur from the error term caused by the time discretization and the cross term. The simulation time presented in Table 3 is normalized by the simulation time of the Gottlieb–Turkel scheme. Consistent with the one-dimensional results, the Runge–Kutta scheme is more computationally efficient, using 16.5% less CPU time.

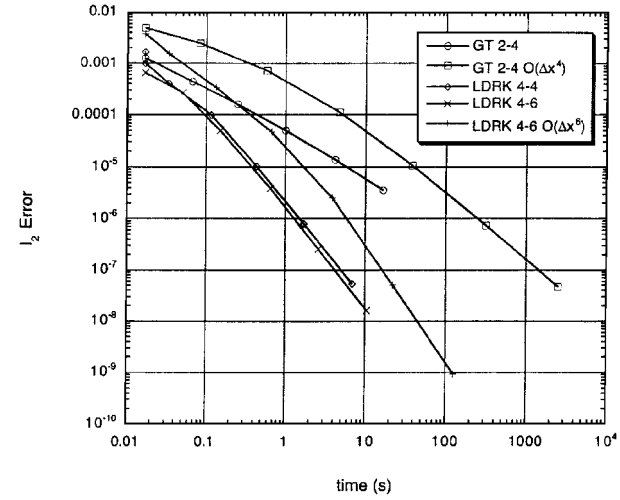

Fig. 14 Efficiency of the numerical schemes for the nonlinear problem.

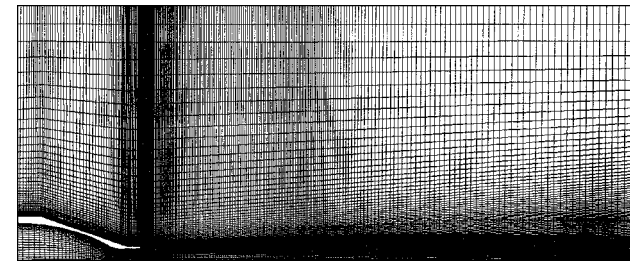

Fig. 15 Computational grid.

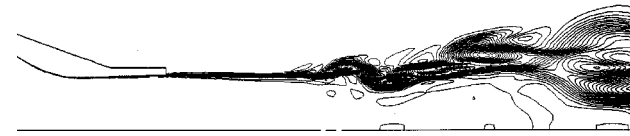

a) Gottlieb–Turkel 2-4

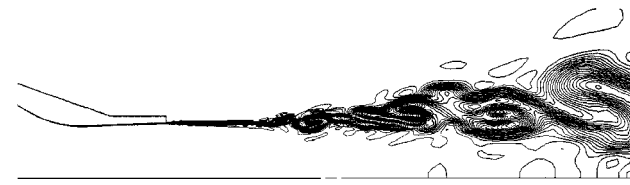

b) Runge–Kutta 4-4

Fig. 16 Entropy contours for the axisymmetric jet.

Conclusions

Two types of high-order numerical schemes suitable for computational aeroacoustics were examined. The Gottlieb–Turkel 2-4 predictor-correctorscheme and two Runge–Kutta schemes (4-4 and 4-6) are used to solve the one-dimensional inviscid convection of a Gaussian pulse. Two cases, linear and nonlinear convection, are examined. The numerical solution was compared to the exact solution to obtain the error. Efficiency of the schemes was determined by comparing the numerical error with the computational cost needed to obtain the solution. For schemes with lower-order time stepping, the truncation error caused by the time stepping dominates the solution for optimum time steps. This reduces the overall error of the scheme to order of the time stepping and eliminates any benefit of the higher-order spatial discretization. Reducing the time step can effectively increase the order of accuracy to that of the spatial discretization. However, this increased accuracy is balanced by an increase in the computational cost. The uniformly fourth-order-accurate Runge–Kutta scheme proves to be superior to the second-order temporal and fourth-order spatial accurate Gottlieb–Turkel scheme in terms of truncation error and computational efficiency. Increasing the spatial accuracy of the Runge–Kutta scheme to sixth order does not improve the efficiency of the scheme.

The Gottlieb–Turkel 2-4 and Runge–Kutta 4-4 schemes are then used to solve the unsteady axisymmetric Navier–Stokes equations for a supersonic jet flow. These two schemes with identical spatial discretization error terms but different temporal and cross-error terms show different solutions in the mixing layer. The Runge–Kutta scheme provides better resolution of large-scale structures and requires less computational time. This result indicates that the time discretization is an important factor for unsteady Navier–Stokes computations such as those performed in DNS and LES analyses.

In general, the temporal and spatial accuracy of a scheme cannot be considered separately, and the error of the scheme is determined by the dominate error term. The problems considered in this study indicate that a numerical scheme with a balance of spatial and temporal errors, such as the Runge–Kutta 4-4 scheme, is a better choice for CAA problems.

References

[1]Morris, P. J., Wang, Q., Long, L. N., and Lockard, D. P., "Numerical Predictions of High Speed Jet Noise," AIAA Paper 97-1598, May 1997.

[2]Zhao, W., Frankel, S. H., and Mongeau, L., "Large Eddy Simulation of Sound Radiation from a Subsonic Turbulent Jet," AIAA Paper 2000-2078, June 2000.

[3]Georgiadis, N. J., Alexander, J. I. D., and Reshotko, E., "Development of a Hybrid RANS/LES Method for Compressible Mixing Layer Simulations," AIAA Paper 2001-0289, Jan. 2001.

[4]Freund, J. B., Lele, S. K., and Moin, P., "Direct Simulation of a Mach 1.92 Jet and Its Sound Field," AIAA/Confederation of European Aerospace Societies Paper 98-2291, June 1998.

[5]Freund, J. B., "Direct Numerical Simulation of the Noise from a Mach 0.9 Jet," *Proceedings of FEDSM'98, 3rd ASME/JSME Joint Fluids Engineering Conference*, San Francisco, 1999, FEDSM99-7251.

[6]Hixon, R., "A New Class of Compact Schemes," AIAA Paper 98-0367, Jan. 1998.

[7]Visbal, M. R., and Gaitonde, D. V., "High-Order Accurate Methods for Unsteady Vortical Flows on Curvilinear Meshes," AIAA Paper 98-0131, Jan. 1998.

[8]Tam, C. K. W., and Webb, J. C., "Dispersion Relation-Preserving Finite Difference Schemes for Computational Aeroacoustics," *Journal of Computational Physics*, Vol. 107, No. 2, 1993, pp. 262–281.

[9]Lele, S. K., "Compact Finite Difference Schemes with Spectral-Like Resolution," *Journal of Computational Physics*, Vol. 103, No. 1, 1992, pp. 16–42.

[10]Vichnevetsky, R., and Bowles, J. B., *Fourier Analysis of Numerical Approximations of Hyperbolic Equations*, Society for Industrial and Applied Mathematics, Philadelphia, 1982.

[11]Hardin, J. C., Ristorcelli, J. R., and Tam, C. K. (eds.), "ICASE/LaRC Workshop on Benchmark Problems in Computational Aeroacoutics (CAA)," NASA CP 3300, May 1995.

[12]Gottlieb, D., and Turkel, E., "Dissipative Two-Four Methods for Time-Dependent Problems," *Mathematics of Computation*, Vol. 30, No. 136, 1976, pp. 703–723.

[13]MacCormack, R. W., "The Effect of Viscosity in Hypervelocity Impact Cratering," AIAA Paper 69-354, April 1969.

[14]Jameson, A., and Baker, T. J., "Multigrid Solution of the Euler Equations for Aircraft Configurations," AIAA Paper 84-0093, Jan. 1984.

[15]Carpenter, M. H., and Kennedy, C. A., "Fourth-Order 2N-Storage Runge-Kutta Schemes," NASA TM 109112, June 1994.

[16]Hu, F. Q., Hussaini, M. Y., and Manthey, J. L., "Low-Dissipation and Low-Dispersion Runge–Kutta Schemes for Computational Acoustics," *Journal of Computational Physics*, Vol. 124, No. 1, 1996, pp. 177–191.

[17]Gottlieb, S., and Chu, C. W., "Total Variation Diminishing Runge–Kutta Schemes," NASA CR 201591, July 1996.

[18]Stanescu, D., and Habashi, W. G., "2N-Storage Low Dissipation and Dispersion Runge–Kutta Schemes for Computational Acoustics," *Journal of Computational Physics*, Vol. 143, No. 12, 1998, pp. 674–681.

[19]Kennedy, C. A., and Carpenter, M. H., "Comparison of Several Numerical Methods for Simulation of Compressible Shear Layers," NASA TP 3484, Dec. 1997.

[20]Panda, J., and Seasholtz, R. G., "Velocity and Temperature Measurement in Supersonic Free Jets Using Spectrally Resolved Rayleigh Scattering," AIAA Paper 99-0296, Jan. 1999.

[21]DeBonis, J. R., "The Numerical Analysis of a Turbulent Compressible Jet," Ph.D. Dissertation, Dept. of Aerospace Engineering and Aviation, Ohio State Univ., Columbus, OH, Dec. 2000.

[22]Courant, R., Friedrichs, K. O., and Lewy, H., "On the Partial Difference Equations of Mathematicsl Physics," *IBM Journal of Research and Development*, Vol. 11, 1967, pp. 215–234.

W. J. Devenport
Associate Editor